A&A 533, A76 (2011)
DOI: 10.1051/0004-6361/201117427

Astronomy & Astrophysics

Small-scale Hα jets in the solar chromosphere

D. Kuridze[1], M. Mathioudakis[1], D. B. Jess[1], S. Shelyag[1], D. J. Christian[2], F. P. Keenan[1], and K. S. Balasubramaniam[3]

[1] Astrophysics Research Centre, School of Mathematics and Physics, Queen's University Belfast, Belfast, BT7 1NN, Northern Ireland, UK
e-mail: dkuridze01@qub.ac.uk
[2] Department of Physics and Astronomy, California State University, Northridge, CA 91330, USA
[3] Air Force Research Laboratory, Solar and Solar Disturbances, Sunspot, NM 88349, USA

Received 7 June 2011 / Accepted 3 August 2011

ABSTRACT

Aims. High temporal and spatial resolution observations from the Rapid Oscillations in the Solar Atmosphere (ROSA) multiwavelength imager on the Dunn Solar Telescope are used to study the velocities of small-scale Hα jets in an emerging solar active region.
Methods. The dataset comprises simultaneous imaging in the Hα core, Ca II K, and G band, together with photospheric line-of-sight magnetograms. Time-distance techniques are employed to determine projected plane-of-sky velocities.
Results. The Hα images are highly dynamic in nature, with estimated jet velocities as high as 45 km s^{-1}. These jets are one-directional, with their origin seemingly linked to underlying Ca II K brightenings and G-band magnetic bright points.
Conclusions. It is suggested that the siphon flow model of cool coronal loops is suitable for interpreting our observations. The jets are associated with small-scale explosive events, and may provide a mass outflow from the photosphere to the corona.

Key words. Sun: activity – Sun: chromosphere – Sun: faculae, plages – Sun: photosphere – Sun: surface magnetism

1. Introduction

The solar chromosphere is permeated by a wide range of highly dynamic features including jets, fibrils, mottles, spicules, Ellerman bombs, and Hα surges. In particular, chromospheric jets are one of the most important, yet also most poorly understood phenomena of the Sun's magnetic atmosphere. Observed chromospheric jet velocities are generally measured to have values of around ~20–40 km s^{-1} (Tsiropoula & Tziotziou 2004; Chae et al. 2000; Lin et al. 2008). Apart from these typical speeds, high velocity flows (>100 km s^{-1}) are also observed in some chromospheric surges and blobs (Foukal 2004; van Noort et al. 2006).

Several previous studies indicate that the energy required to drive these chromospheric jets can be released by magnetic reconnection occurring low in the solar atmosphere (Canfield et al. 1996; Chae et al. 2003; Chae 2007; Shibata et al. 2007). Yoshimura et al. (2003) found a close correlation between Hα surges, Transition Region and Coronal Explorer (TRACE) brightenings in the 1600 Å waveband, and magnetic flux cancellations surrounding ephemeral regions. More recently, Morita et al. (2010) observed chromospheric anemone jets in Ca II K_1 and K_2 lines as intensity peaks in the light curves. They also found cancellation of magnetic flux near the jet area. These results strongly suggest that chromospheric jets may be generated by magnetic reconnection, similar to what occurs on a larger scale in the corona. Also, the multi-wavelength studies of Yoshimura et al. (2003) and Brooks et al. (2007) indicate that chromospheric surges are indeed driven by magnetic reconnection. Alternatively, Hansteen et al. (2006) suggest that the formation of jets, linked to dynamic fibrils, mottles and spicules, could be driven by magneto-acoustic shocks that leak upward through the chromosphere as a result of convective flows in the photosphere and global p-mode oscillations.

Recently, a multi-wavelength study involving Solar Dynamic Observatory (SDO) and Hinode observations has highlighted the importance of chromospheric jets and spicules for providing the mass supply for the corona (De Pontieu et al. 2011). However, spectroscopic observations can only provide the line-of-sight (LOS) component of velocity, with any small-scale Doppler phenomena cancelling out if the spatial resolution is not sufficiently high. To investigate the small-scale structure, here we present high spatial and temporal resolution observations of an emerging active region in Hα core, Ca II K, G band, and LOS magnetograms. In the following sections, we describe the details of the observations and the image processing (Sect. 2), the analysis, and results (Sect. 3), and finally discuss and summarise possible interpretations of our findings (Sect. 4).

2. Observations and data reduction

The observations were obtained between approximately 15:00–16:00 UT on 2009 May 31 with the Rapid Oscillations in the Solar Atmosphere (ROSA; Jess et al. 2010b) imaging system, mounted on the Dunn Solar Telescope (DST) at the National Solar Observatory, New Mexico, USA. High-order adaptive optics were used throughout the observations. The photospheric target under investigation comprises a multitude of magnetic pores and associated faculae, located at heliocentric coordinates (−540″, 435″). Our dataset includes simultaneous imaging in the G band, Hα core, Ca II K, and LOS magnetograms. A spatial sampling of 0.069″/pixel was selected, matching the diffraction limit of the DST to that of the G band, resulting in a field-of-view of approximately 69″ × 69″.

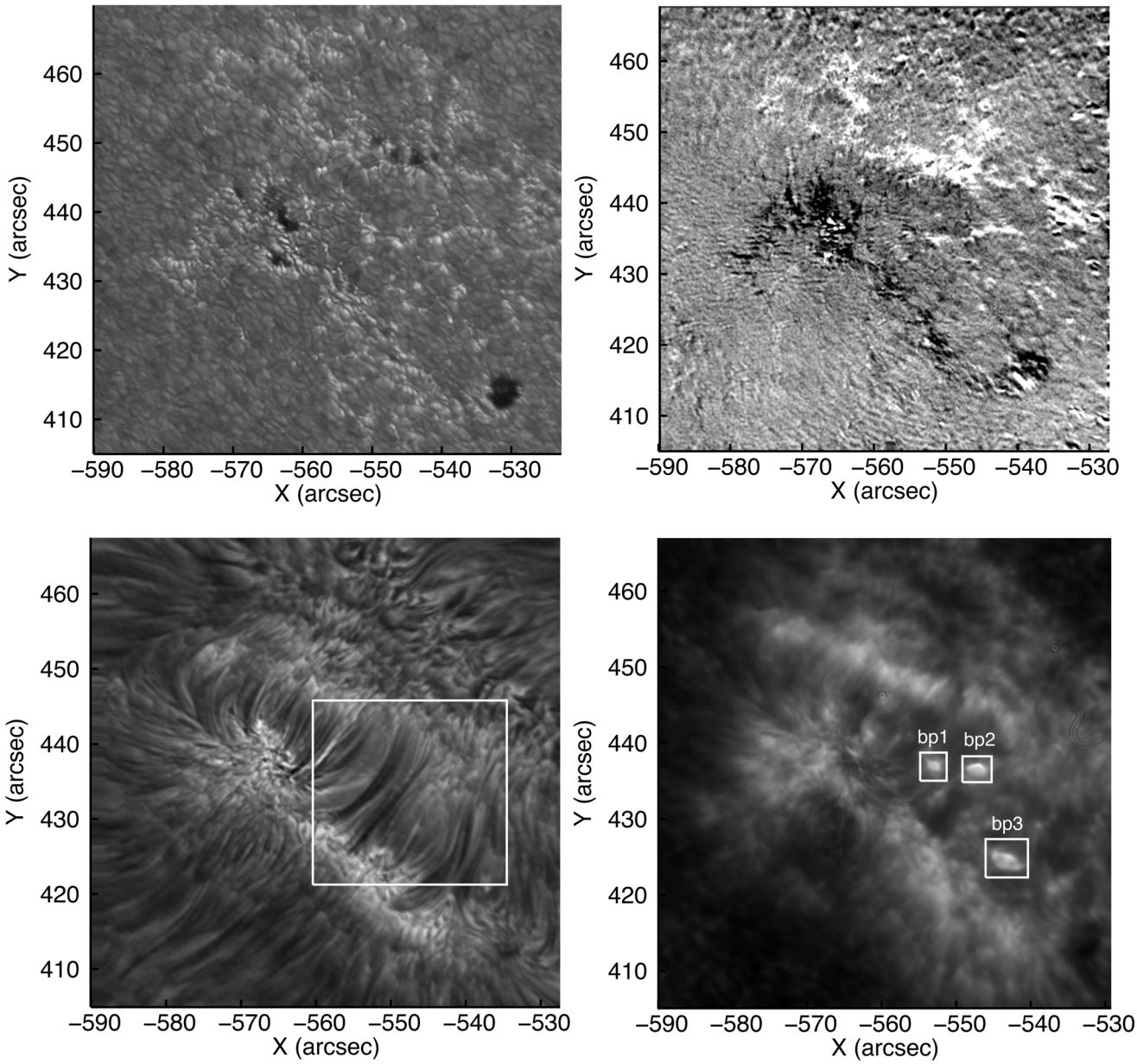

Fig. 1. Simultaneous ROSA images of the G band (*top left*), line-of-sight magnetogram (*top right*), Hα core (*bottom left*), and Ca II K core (*bottom right*). The magnetogram colour scale is in Gauss, where white indicates positive magnetic polarities, while black demonstrates polarities which are negative. Artificial saturation at ±400 G is implemented to highlight regions of weak magnetic polarity on the solar surface. The white rectangle in the Hα core image indicates the approximate position where most of the jets are observed. White rectangles in the Ca II K image, identified by "bp1", "bp2", and "bp3", are the bright points selected for temporal analysis. Axes are in heliocentric arcseconds, where $1'' \approx 725$ km.

The images obtained were processed with speckle reconstruction algorithms (Wöger et al. 2008), with the removal of large-scale seeing distortions achieved by destretching the data relative to simultaneous high-contrast continuum images. The algorithms utilised 32 images per reconstruction, resulting in an effective cadence of 8.4 s for Hα, Ca II K, and LOS magnetograms, while the reconstructed G-band cadence was 1.1 s. Magnetograms were constructed as normalised to their sum difference images of left- and right-hand circularly polarised light obtained 125 mÅ into the blue wing of the magnetically-sensitive Fe I absorption line at 6302.5 Å. A blue-wing offset was required to minimise granulation contrast, while conversion of the filtergram into units of Gauss was performed using simultaneous SoHO/MDI magnetograms (see discussion in Jess et al. 2010a). ROSA images in G band, Hα core, Ca II K, and LOS magnetograms are shown in Fig. 1.

3. Analysis and disscussion

The area under investigation (see boxed region in the lower left panel of Fig. 1) consists of a multitude of highly dynamic thread-like structures, which connect areas of opposite magnetic polarity, forming a "chromospheric arcade".

A thorough examination of the Hα core images reveals a total of 27 jet-like structures, some of which are displayed in Fig. 2. The velocities of the jets are determined using space-time slices (x–t plots), generated along the path of the jet trajectories (Fig. 3). Velocity estimates for these jets are in the range 20–45 km s^{-1}, with a histogram of their occurrence plotted in Fig. 4. Detailed properties for the six most prominent jets (see Fig. 2) are listed in Table 1.

Almost half of the Hα jets originate from locations co-spatial with Ca II K and G-band bright points. Three examples of bright

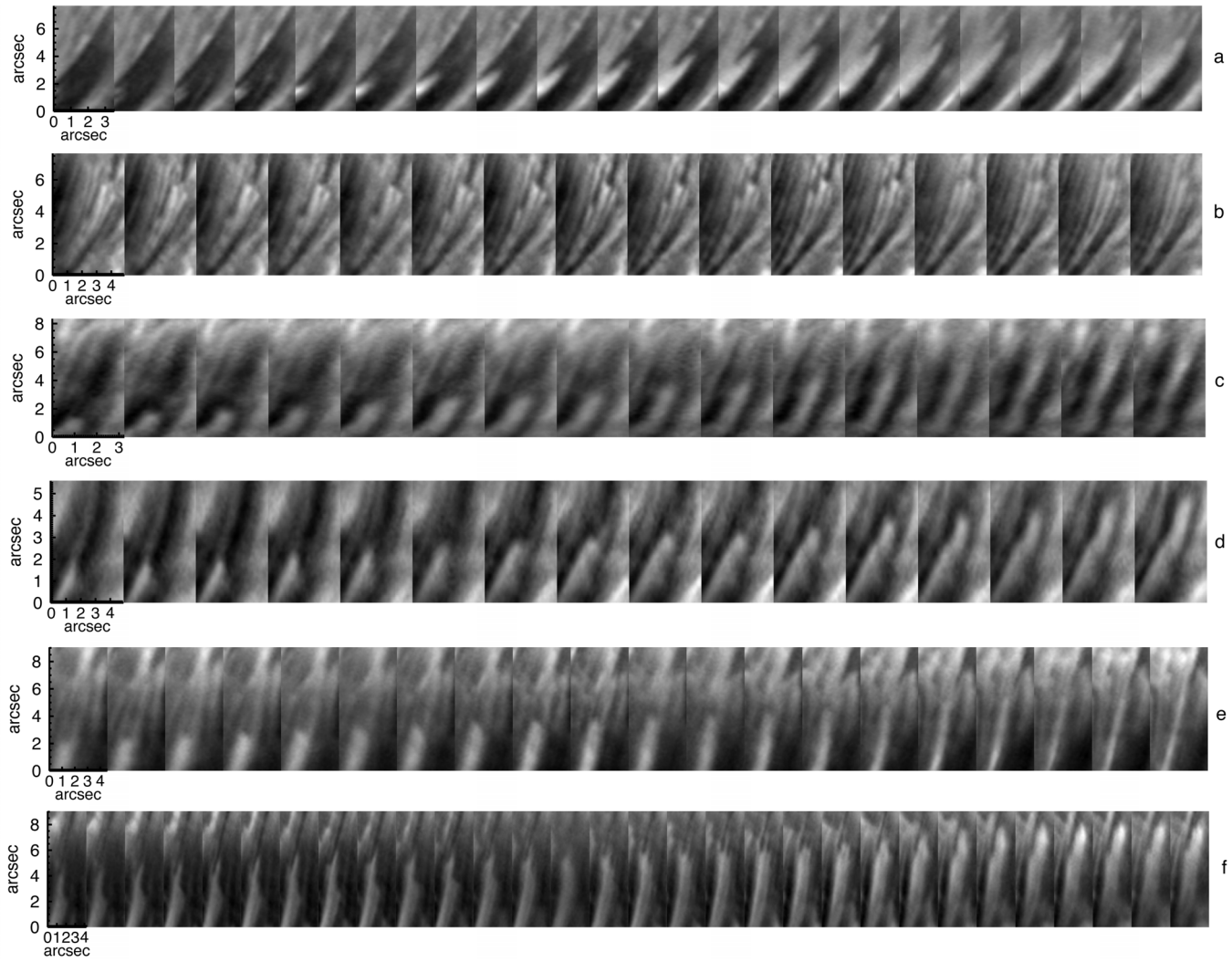

Fig. 2. Six examples of Hα jets observed within the white rectangle in the lower left panel of Fig. 1. Each successive image is separated by a time of 8.4 s, while the length of the jet structures range between approximately 3000–6000 km.

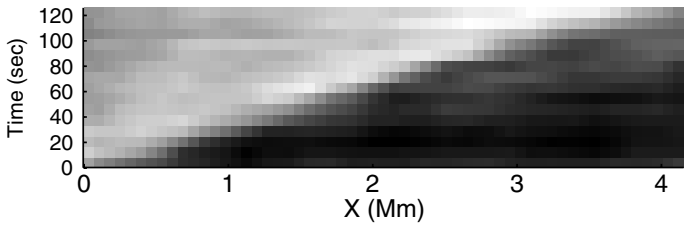

Fig. 3. Hα time-distance diagram of jet *a*, taken from Fig. 2. The gradient of the diagonal ridge in this *x*–*t* slice corresponds to the jet velocity. The velocity of this jet is 34 km s^{-1}.

points are outlined in the lower right panel of Fig. 1 using white rectangles and labelled as "bp1", "bp2", and 'bp3'. All six jets shown in Fig. 2, as well six additional jets, are co-spatial with these bright features, and the evolution of the Ca II K bright point intensities indicates a possible correlation with the Hα jets. Ca II K intensity enhancements and strong isolated peaks are visible in the bright point light curves shown in Fig. 5. In the light curve of bp1 (top panel), the strongest peak around 15:20 UT is followed by three Hα jets occurring at ~15:21, 15:24, 15:26 UT (crosses). From 15:29, there is no significant enhancement in the Ca II K intensity and correspondingly no Hα events. There is an enhanced intensity for the first few minutes in the light curve of bp2. During this time interval, four strong Hα jets are generated at the location of bp2. Furthermore, one of the most isolated intensity peaks in the light curve of bp2 is around 15:25, and there is an Hα jet observed very close to that time. Two other jets associated with the bp2 occur between 15:31 and 15:33. A sharp decrease in the intensity of bp2 occurs after this time. In the light curve of bp3, the peaks are located at around 15:10 and 15:18 UT. The eruption of two jets (e, f in Fig. 2) are observed near these peaks. Hα jets appear to initiate at times when the Ca II K intensity rises, suggesting a possible link between the two phenomena. It must be noted that there are some bright peaks in the light curves of considered bright points (Fig. 5) that are not accompanied by Hα jet events. In these cases the jets may not be visible due to overlapping Hα structures. The remaining jets, of the 27 analysed in this work, also correspond to Ca II K brightenings, however, these brightenings are not observed as localised, simple, fine areas, and makes them somewhat more difficult to disentangle.

Observed 27 jets are initiate in about 9 distinct, small-scale (~5″×5″) regions. As we have already mentioned, almost half of

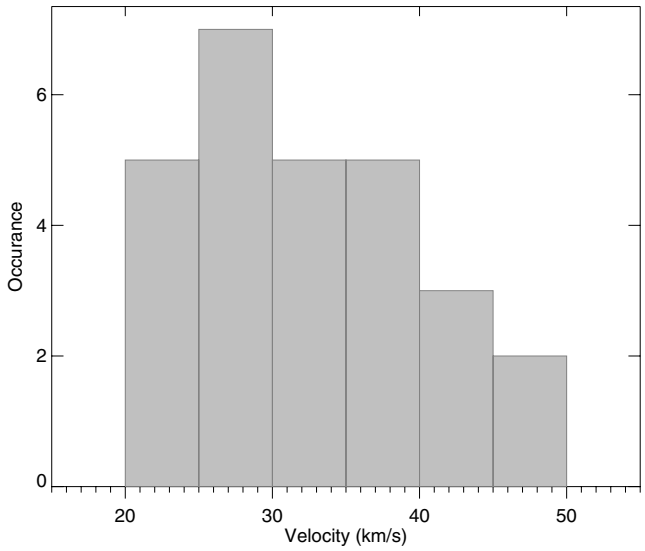

Fig. 4. Velocity distribution of the 27 Hα jets.

Table 1. Detailed parameters of the jets displayed in Fig. 2.

Event name	Starting time (UT)	Duration of the event (s)	Velocity (km s^{-1})
Jet a	15:24:46	160	34
Jet b	15:03:53	142	20
Jet c	15:31:36	135	35
Jet d	15:33:08	145	38
Jet e	15:18:20	177	21
Jet f	15:05:27	250	23

them originate from the three bright points labelled in the bottom right panel in Fig. 1. This fact indicates repetitive nature of the observed jets, however, no well-defined period was found.

Light curves of background quiescent Ca II K regions do not indicate any intensity peaks or significant enhancements. We note that small amplitude intensity fluctuations consistent with the well-known 3–5 min acoustic modes are observed in the both the quiescent and bright point regions (see e.g. Fleck & Schmitz 1991; Kariyappa et al. 2001). However, the intermittent nature of the jets and their supersonic velocities suggest that they are not associated with the acoustic mode oscillations.

Striking similarities between Hα core observations and TRACE Fe IX/X images suggest that Hα may be used as a proxy for coronal material. These similarities may be attributed to reduced Hα opacity, excess emissivity, or a combination of both (Rutten 2007). A cool loop model may therefore be appropriate for chromospheric structures.

Doyle et al. (2006) suggested that one-directional plasma flow in a cold coronal loop (10^5–10^6 K) can be interpreted in terms of a short-lived siphon flow which may arise due to a non-linear heating pulse at one of the loop footpoints. The supersonic flow velocities are determined by the duration of the pulse, in addition to its associated energy input. All our presented Hα jets are one-directional, and propagate from negative (bottom portion of the white rectangle in the lower left panel of Fig. 1) to positive polarities (upper section of the white rectangle in the lower left panel of Fig. 1). The established supersonic velocities are very similar to those predicted by the siphon flow model. Furthermore, other similarities between

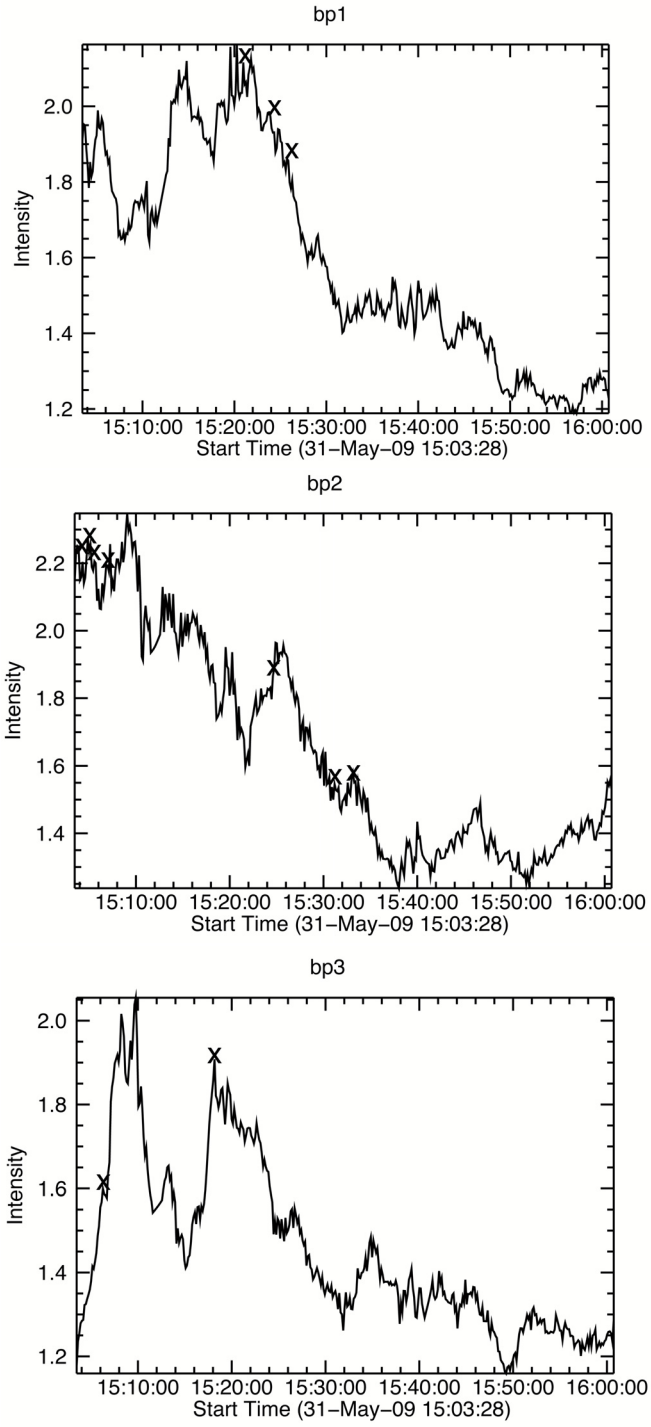

Fig. 5. Light curves of the Ca II K bright points outlined with rectangles in the lower right panel of Fig. 1. "x" symbols indicate the time when a jet event originated from that particular bright point.

observations of Doyle et al. (2006) and our findings, such as the comparable time scales of the observed events and also morphological similarities of the observed structures motivated us to interpret our observation by means of siphon flow model. We note that Uitenbroek et al. (2006) used spectroheliograms of the Ca II IR triplet (8542.1 Å) to detect a siphon flow associated with a magnetic pore. Line of sight velocities as high as 27 km s^{-1} were detected.

Using the heating rate and plasma flow velocity given by the coronal loop simulation of Doyle et al. (2006), we can estimate that the rate of energy conversion from the source to the kinetic energy of the flow in the loop is ∼0.1. This estimate is based on an ambient coronal density of 10^{-13} g cm^{-3}. If we assume (i) that the same rate applies in the chromosphere, (ii) a chromospheric density of 10^{-11} g cm^{-3} and (iii) the chromospheric jet velocity of 40 km s^{-1} as estimated from the observations, we obtain the total heating energy of about 10 erg cm^{-3}. Assuming the duration of energy release in the chromospheric loop footpoint of the order of ten seconds, we obtain a heating rate $h \sim 1$ erg cm^{-3} s^{-1}, a value significantly higher than the one estimated for the coronal loop. This is not surprising as more energy is required to propel the denser chromospheric jets to velocities comparable to those in the coronal model. The volume of the Ca II K bright points (bottom right panel of the Fig. 1), which are the footpoints of the Hα jets, can be estimated as 10^{24} cm^3 (assuming a size of approximately $2'' \times 2''$ and a height of $\sim 1''$). Thus, the estimated released energy for the heating rate calculated above is about 10^{24} erg. The total mass of the jet ($\sim 10^{12}$ g) is estimated from the chromospheric density and average volume of the jet. In order to bring the total mass up to a height of about 1.5×10^3 km an energy of $\sim 10^{24}$ erg is needed. These values are comparable to the estimated energy stored in the bright point volume. We emphasise that the above estimates are approximate and a detailed simulation is required to account for all processes involved in this energy release.

4. Concluding remarks

We present evidence for small-scale, one directional Hα jets in the solar chromosphere. Jet velocities as high as 45 km s^{-1} are found. Observation shows the relations between Hα jets and Ca II K bright points. We interpret this phenomena by means of a coronal loop siphon flow model, whereby one of the loop footpoints is driven by a localised, non-linear heating pulse (Doyle et al. 2006). The energy required to drive jets is estimated as 10^{24} erg.

The jets presented here appear to be associated with small-scale explosive events, and may provide a mechanism to support mass outflow from the chromosphere out into the corona.

Acknowledgements. Observations were obtained at the National Solar Observatory, operated by the Association of Universities for Research in Astronomy, Inc (AURA) under agreement with the National Science Foundation. This work is supported by the Science and Technology Facilities Council (STFC), with D.B.J. particularly grateful for the award of an STFC post-doctoral fellowship. We thank the Air Force Office of Scientific Research, Air Force Material Command, USAF for sponsorship under grant number FA8655-09-13085.

References

Brooks, D. E., Kurokawa, H., & Berger, T. E. 2007, ApJ, 656, 1197
Canfield, R. C., Reardon, K. P., Leka, K. D., et al. M. 1996, ApJ, 464, 1016
Chae, J. 2007, in New Solar Physics with Solar-B Mission, ed. K. Shibata, S. Nagata, & T. Sakurai (San Francisco, CA: ASP), ASP Conf. Ser., 369, 243
Chae, J., Denker, C., Spirock, T., Wang, H., & Goode, P. 2000, Sol. Phys., 195, 333
Chae, J., Moon, Y.-J., & Park, S.-Y. 2003, JKAS, 36, S13
De Pontieu, B., McIntosh, S.W., Carlsson, M., et al. 2011, Science, 331, 55
Doyle, J. G., Taroyan, Y., Ishak, B., Madjarska, M. S., & Bradsgaw, S. J. 2006, A&A, 452, 1075
Fleck, B., & Schmitz, F. 1991, A&A, 250, 235
Foukal, P. 2004, Solar Astrophysics, 2nd edn. (Weinheim: Wiley-VCH)
Hansteen, V. H., De Pontieu, B., Rouppe van der Voort, L., van Noort, M., & Carlsson, M. 2006, ApJ, 647, L73
Jess, D. B., Mathioudakis, M., Christian, D. J., et al. 2010a, ApJ, 719, L134
Jess, D. B., Mathioudakis, M., Christian, D. J., et al. 2010b, Sol. Phys., 261, 363
Kariyappa, R., Varghese, B. A., & Curdt, W. 2001, A&A, 374, 691
Lin, Y., Martin, S. F., Engvold, O., et al. 2008, Adv. Space Res., 42, 803
Morita, S., Shibata, K., Ueno, S., et al. 2010, PASJ, 62, 901
Rutten, R. J. 2007, ASP Conf. Ser. 368, ed. P. Heinzel, I. Dorotovic, & R. J. Rutten, San Francisco, 27
Shibata, K., Nakamura, T., Matsumoto, T., et al. 2007, Science, 318, 1591
Tsiropoula, G., & Tziotziou, K. 2004, A&A, 424, 279
Uitenbroek, H., Balasubramaniam, K. S., & Tritschler, A. 2006, ApJ, 645, 776
van Noort, M., & Rouppe van der Voort, L. 2006, ApJ, 648, L67
Wöger, F., von der Lühe, O., & Reardon, K. 2008, A&A, 488, 375
Yoshimura, K., Kurokawa, H., Shimojo, M., & Shine, R. 2003, PASJ, 55, 313